

Towards Quantum Resolution Limit of Magnetic Field Imaging with Nitrogen-Vacancy Centers

Nico Deshler^{1,*}, Ayan Majumder², Kasturi Saha², and Saikat Guha¹

¹Wyant College of Optical Sciences, University of Arizona

²Department of Electrical Engineering, Indian Institute of Technology Bombay

*ndeshler@arizona.edu

Abstract: Nitrogen-vacancy centers are an emerging platform for optically interrogating spatially-varying magnetic fields. We calculate the quantum Fisher information matrix pertaining to the positions and local magnetic fields of two nitrogen-vacancy centers under the ODMR protocol. © 2024 The Author(s)

1. Introduction

The Quantum Diamond Microscope (QDM) uses Optically-Detected Magnetic Field Resonance (ODMR), which exploits the electronic energy-level structure of nitrogen-vacancy (NV) centers in diamond crystal lattices to image spatially-varying magnetic fields. In continuous-wave ODMR, an optical pump laser drives transitions between the ground and excited state of a NV center while a microwave frequency-scan probes for spin-level energy splitting induced by the presence of a weak external magnetic field (Zeeman effect). The optical photon emission rate of a NV center varies as a function of the microwave frequency according to a parametric model that depends on the local magnetic field strength. Pre-detection adaptive spatial mode sorting is known to resolve mutually-incoherent clusters of point-emitters at sub-Rayleigh separations more accurately than conventional focal plane imaging [1]. Hence, we argue that spatial mode sorting must also yield a higher-resolution QDM. We derive the quantum Fisher information matrix (QFIM) for spatially localizing (resolving) two closely-spaced NV centers and estimating the magnetic field strengths at their respective locations. Our results suggest that a two-stage strategy comprised of spatial mode sorting for NV localization followed by direct imaging ODMR for magnetic field estimation is nearly quantum-optimal, and would significantly outperform a conventional QDM with respect to the spatial resolution of the magnetic field.

2. Theory

We consider two identical NV centers separated by a distance s on the sample plane such that their geometric center is aligned with the optical axis of the imaging system (Fig. 1(a)). Under the ODMR protocol, each NV center ($j = 1, 2$) emits photons at a rate $I_j(\omega) := -c[(L(\omega; -\Delta_j) + L(\omega; +\Delta_j))/2 - 1]$, where ω is the microwave frequency, Δ_j is the detuning frequency of the Zeeman splitting energy, c is a constant of units [photons/sec], and $L(\cdot)$ is a dimensionless Lorentzian function $L(\omega; \Delta) := \frac{1}{1 + (\omega - \omega_0 - \Delta)^2/w^2}$ (Fig. 1(b)). The Lorentzian involves the zero-field frequency ω_0 and the response linewidth w . The detuning frequency Δ_j encodes the local magnetic field magnitude B_j along the NV-axis through $\Delta_j = \sqrt{((g\mu_B/\hbar)B_j)^2 + E^2}$, [2, 3] where $g \approx 2.0$ is the g-factor, μ_B is the Bohr magneton, \hbar is the reduced Planck constant, and E is the off-axis zero-field splitting factor induced by strain in the diamond lattice. We find the quantum Fisher information matrix (QFIM) for the parameter vector $\theta = [s, \Delta_1, \Delta_2]^T$ from the standard formulation of the 2-source optical quantum state [4], $\hat{\rho}(\omega) = b(\omega)|\psi_1\rangle\langle\psi_1| + (1 - b(\omega))|\psi_2\rangle\langle\psi_2|$, where $b(\omega) := \frac{I_1(\omega)}{I_1(\omega) + I_2(\omega)}$ is the relative brightness of the two NV centers at a given microwave frequency, and $|\psi_{1,2}\rangle = |\psi(x \pm s/2)\rangle$ are single-photon states of the shifted point-spread function (PSF) $\psi(x)$. Extending previous results on the QFIM for two incoherent point sources [5], we find the non-zero entries of the *per-photon* QFIM for the parameters θ to be,

$$Q_{ij}(\omega) = \begin{cases} p^2 & i, j = 0, 0 \\ + (1 - \delta^2) b(\omega) (1 - b(\omega)) \left(\frac{\partial_{\Delta_j} I_i(\omega)}{I_i(\omega)} \right)^2 & i, j > 0 \text{ and } i = j \\ - (1 - \delta^2) b(\omega) (1 - b(\omega)) \left(\frac{\partial_{\Delta_j} I_i(\omega)}{I_i(\omega)} \right) \left(\frac{\partial_{\Delta_i} I_j(\omega)}{I_j(\omega)} \right) & i, j > 0 \text{ and } i \neq j, \end{cases} \quad (1)$$

where $p^2 := -\int_{-\infty}^{\infty} \psi^*(x) \partial_x^2 \psi(x) dx$ and $\delta := \int_{-\infty}^{\infty} \psi^*(x) \psi(x - s) dx$.

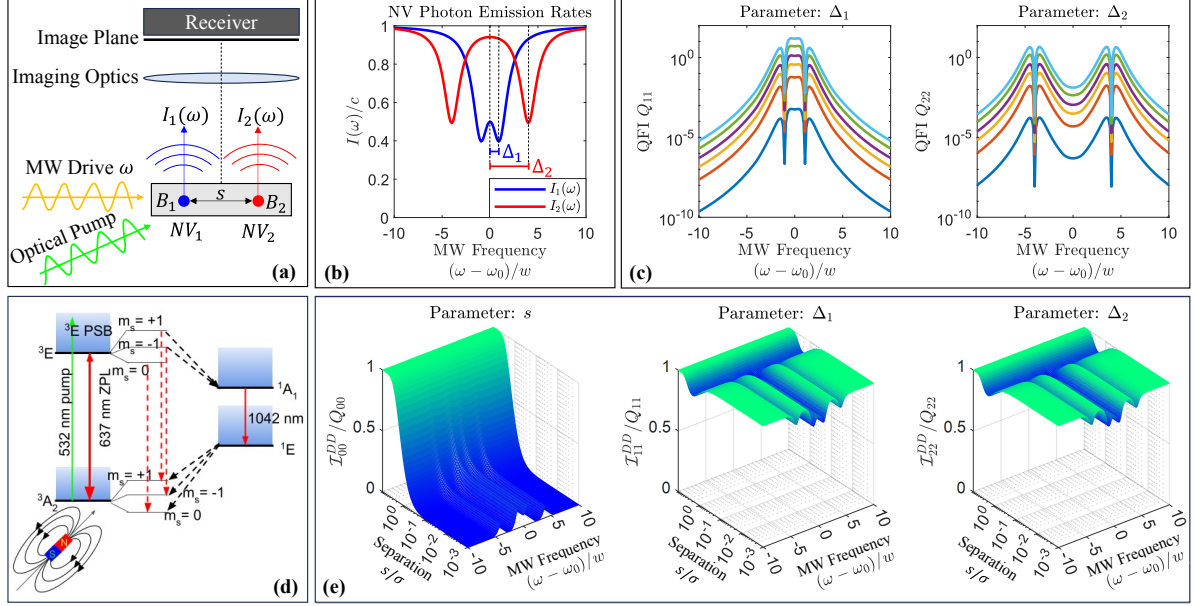


Fig. 1. (a) Schematic of the ODMR protocol for a diamond sample consisting of two NV centers. (b) Emission rates from the NV centers with $\Delta_1/w = 1$ and $\Delta_2/w = 4$. (c) QFI of the detuning parameters as a function of microwave drive frequency for separations $s/\sigma = [.01, .1, .25, .5, 1, 2]$ (bottom to top). (d) Electronic energy level diagram of a NV center in the presence of an external magnetic field. Without the magnetic field $m_s = \pm 1$ states are degenerate. (e) Direct detection CFI as a fraction of the QFI for each estimation parameter.

3. Results and Outlook

We assume a Gaussian PSF: $\psi(x) = (2\pi\sigma^2)^{-1/4} \exp(-x^2/4\sigma^2)$, $p^2 = 1/4\sigma^2$, and $\delta = \exp(-s^2/8\sigma^2)$. Since the QFI for Δ_1, Δ_2 is globally modulated by $1 - \delta^2$, the minimum achievable uncertainty (variance) for B_1, B_2 grows as $\sim 1/s^2$ for sub-Rayleigh NV separations as shown by the variation in spacing between QFI curves in Fig. 1(c). In Fig. 1(e) we show the classical Fisher information (CFI) of direct detection (DD) \mathcal{I}_{ij}^{DD} as a fraction of the QFI for each parameter. If the emitters are well-separated ($s \gg \sigma$), then DD saturates the QFI for all parameters. Otherwise, if the emitters are unresolved ($s \ll \sigma$), then DD is severely sub-optimal for estimating separation s , yet remains nearly optimal for estimating Δ_1, Δ_2 . This suggests that first using a PSF-adapted spatial mode demultiplexer (PAD-SPADE) to estimate s [4], followed by direct imaging ODMR to estimate Δ_1, Δ_2 , would lead to higher-resolution magnetic-field imaging compared to a conventional QDM. Extending this insight to a dense cluster of NV centers, an adaptive measurement strategy that alternates between re-configurable modal imaging and direct-imaging ODMR may offer similar resolution improvements. The QFIM also points to possible optimization of the ODMR scanning schedule. Assuming a fixed scan-time budget, one may architect a probability density $f(\omega)$ over the scanning domain $[\omega_i, \omega_f]$ such that the composite QFIM $\mathbf{Q} = \int_{\omega_i}^{\omega_f} f(\omega)(I_1(\omega) + I_2(\omega))\mathbf{Q}(\omega)$ is maximized with respect to an objective function (e.g. $\text{Tr } \bar{\mathbf{Q}}$). This amounts to prioritizing (lingering at) particular microwave frequencies in order to maximize the total information collected over the allotted scanning period. Future work will compare simulated magnetic-field images different receiver designs, derive information-optimal ODMR scheduling, assess coherence (and quantum interference) effects among NV emissions, and address real-world non-idealities.

References

1. K. K. Lee, C. N. Gagatsos, S. Guha, and A. Ashok, "Quantum-inspired Multi-Parameter adaptive bayesian estimation for sensing and imaging," *IEEE J. Sel. Top. Signal Process.* pp. 1–11 (2022).
2. L. Rondin, J.-P. Tetienne, T. Hingant, J.-F. Roch, P. Maletinsky, and V. Jacques, "Magnetometry with nitrogen-vacancy defects in diamond," *Reports on progress physics* **77**, 056503 (2014).
3. J. F. Barry, J. M. Schloss, E. Bauch, M. J. Turner, C. A. Hart, L. M. Pham, and R. L. Walsworth, "Sensitivity optimization for nv-diamond magnetometry," *Rev. Mod. Phys.* **92**, 015004 (2020).
4. M. Tsang, R. Nair, and X.-M. Lu, "Quantum theory of superresolution for two incoherent optical point sources," *Phys. Rev. X* **6**, 031033 (2016).
5. J. Řehaček, Z. Hradil, B. Stoklasa, M. Paúr, J. Grover, A. Krzic, and L. L. Sánchez-Soto, "Multiparameter quantum metrology of incoherent point sources: Towards realistic superresolution," *Phys. Rev. A* **96**, 062107 (2017).